Molecular and Cellular Neuroscience 40 (2009) 328–337

Contents lists available at ScienceDirect

Molecular and Cellular Neuroscience

journal homepage: www.elsevier.com/locate/ymcne

# Formation of posterior cranial placode derivatives requires the *Iroquois* transcription factor *irx4a*

Carmen Gloria Feijóo [a,b], Marioli P. Saldias [a], Javiera F. De la Paz [a], José Luis Gómez-Skarmeta [c], Miguel L. Allende [a,*]

[a] Center for Genomics of the Cell, Facultad de Ciencias, Universidad de Chile, Casilla 653, Santiago, Chile
[b] Departamento de Ciencias Biologicas, Facultad de Ciencias de la Salud, Universidad Andres Bello, Santiago, Chile
[c] Centro Andaluz de Biología del Desarrollo, Consejo Superior de Investigaciones Científicas and Universidad Pablo de Olavide, Sevilla, Spain

ARTICLE INFO

*Article history:*
Received 28 March 2008
Revised 2 September 2008
Accepted 17 November 2008
Available online 6 December 2008

*Keywords:*
Iroquois
Homeobox transcription factor
Trigeminal ganglion
Lateral line

ABSTRACT

Members of the *Iroquois* (*Irx*) homeodomain transcription factor gene family have been implicated in a variety of early developmental processes, including neural pre-patterning, tissue differentiation, neural crest development and cranial placode formation. Here, we report that, in zebrafish, the *irx4a* gene participates in specification of a number of placode derivatives that arise from the posterior placodal field. Specifically, differentiation of the trigeminal, epibranchial and lateral line placodes are affected when *irx4a* function is interrupted using antisense morpholino oligonucleotides. We show that both in the trigeminal ganglion and in the lateral line, *irx4a* is involved in controlling the number of sensory cells that develop. Other phenotypes observed in morphant embryos include misspecification of the heart chambers and failure of retinal ganglion and photoreceptor cell differentiation, functions described previously for *Irx4* in other species. We also provide evidence that *irx4a* regulates the expression of the *sox2* gene, both in the neural plate and in progenitor cells of the lateral line system. Our results point to *irx4a* as a critical gene for numerous developmental processes and highlight its role in the formation of placodal derivatives in vertebrates.


## Introduction

Ectodermal placodes consist of epithelial thickenings that form at characteristic positions anterior and lateral to the head of vertebrate embryos (reviewed in Schlosser, 2005, 2006). They are essential for the formation of the sensory nervous system and their derivatives include ciliated sensory receptors, sensory neurons, neuroendocrine and endocrine cells, the lens, glia and other supporting cells. Placodal cells give rise to the majority of neurons that form the cranial sensory nervous system and contribute to form the cranial ganglia and the specialized sense organs associated with hearing, balance, olfaction and vision. In fish and aquatic amphibians, the trigeminal, lateral line (anterior and posterior), otic and epibranchial placodes become distinct after neural tube closure. The latter three placodes derive from a single ectodermal domain termed the posterior placodal area (Schlosser and Ahrens, 2004). Signaling pathways that have been implicated in induction of these placodes are BMPs, Wnts, FGF, and retinoic acid (Garcia-Castro et al., 2002; Monsoro-Burq et al., 2003; Brugmann et al., 2004). It remains unclear how these signaling pathways are able to activate distinct developmental programs that specify each of the sensory systems. One family of transcription factors that has been linked to maintenance of the posterior placodal field and promotion of the neurogenic fate in specific placodes are the *Iroquois* (*Irx*) genes. Expression analysis in *Xenopus* has shown that the genes *Xiro1*, *Xiro2* and *Xiro3* are expressed in the trigeminal, lateral line, otic and epibranchial domains, both before and after these placodes become distinct (Gómez-Skarmeta et al., 1998; Bellefroid et al., 1998; Glavic et al., 2004; Schlosser and Ahrens, 2004). Inhibition of *Xiro1* activity by dominant negative variants induced at the late gastrula stage produces inhibition of general pre-placodal markers such as *six1*, as well as in the expression of specific placode markers such as *sox2* and *pax2*, without affecting neural plate genes (Glavic et al., 2004). In a similar way, in zebrafish, knockdown of *Irx* function revealed an essential role for this family of genes in the determination of neurons in the trigeminal placodes (Itoh et al., 2002). Expression of several *Irx* family members has been described in posterior placodes or their derived ganglia in zebrafish, including *irx1a*, *irx1b*, *irx2a*, *irx4a*, *irx4b*, *irx5b* and *irx7* (Lecaudey et al., 2005). It has thus been suggested that *Irx* genes, perhaps together with genes of the *sox1b* family, define a posterior equivalence group of placodes (Schossler, 2006).

The *Irx* genes encode a family of Homeoproteins, conserved during evolution, showing parallel functions between invertebrates and vertebrates. During early development, these genes define the identity of large territories and later they have a role in the subdivision of these territories into sub-domains (Cavodeassi et al., 2001; Gómez-Skarmeta and Modolell, 2002). There are three *Iroquois* genes in *Drosophila* (Gómez-Skarmeta and Modelell, 1996), six in the mouse

* Corresponding author. Fax: +56 2 276 3802.
*E-mail addresses:* allende@uchile.cl, allende.miguel@gmail.com (M.L. Allende).

1044-7431/$ – see front matter © 2008 Elsevier Inc. All rights reserved.
doi:10.1016/j.mcn.2008.11.003

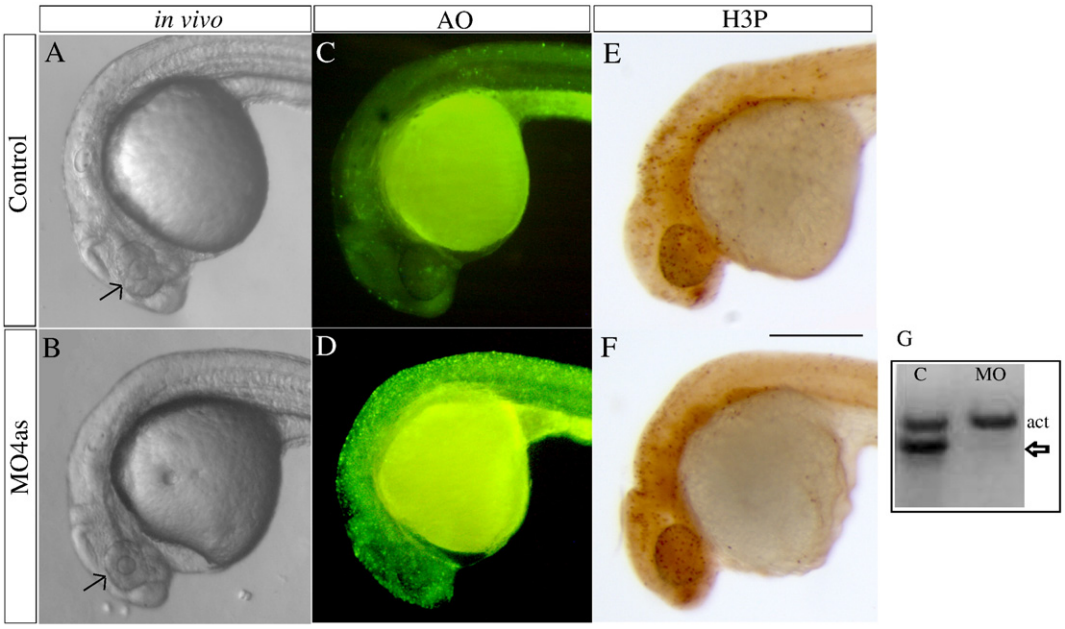


**Fig. 1.** *irx4a* morphant embryos show defects in head size and extensive cell death. (A, B) Images of live wild type (A) and morphant (B) embryos at 24 hpf; Compare the size of the eyes and head (arrows). (C, D) Acridine orange staining of wild type (C) and *irx4a* morphant (D) embryos viewed at 24 hpf. Note the increased number of labeled cells in the morphant embryo (E, F) MO4as injected embryos do not show substantial changes in cell proliferation as evidenced by anti-phospho-histone H3 (H3-P) immunostaining. (G) RT-PCR showing the effect of the MO4as on *irx4a* transcript splicing. RNA prepared from uninjected embryos ("C") shows the internal control band (actin, act) but the absence of unprocessed irx4a mRNA. The presence of this band in MO4as injected fish (arrow) indicates defective *irx4a* mRNA splicing. Panels A–F show lateral views of 24 hpf embryos; dorsal is up, anterior is left. Scale bar in F: 70 μm.

(Bosse et al., 2000; Peters et al., 2000) and eleven in zebrafish (Feijóo et al., 2004; Dildrop and Rüther, 2004). In the genome, the *Iroquois* genes are arranged in clusters, the *Iro* complex (Iro-C) in *Drosophila* and the *Irx* complexes in vertebrates (Gómez-Skarmeta and Modolell, 1996; Peters et al; 2000; Dildrop and Rüther, 2004; Feijóo et al., 2004). Interestingly, the expression patterns of genes within a cluster are highly similar, suggestive of conserved regulatory sequences in the surrounding genomic region (Gómez-Skarmeta and Modelell, 1996, Lecaudey et al., 2005; de la Calle-Mustienes et al., 2005). Moreover, the orthologs of different *Irx* genes among different vertebrates show equivalent expression patterns in several tissues.

In the present study, we have investigated the function of the zebrafish *Irx* family member, *irx4a*. We focus on the role of this gene in specification and neurogenesis during development of the hindbrain

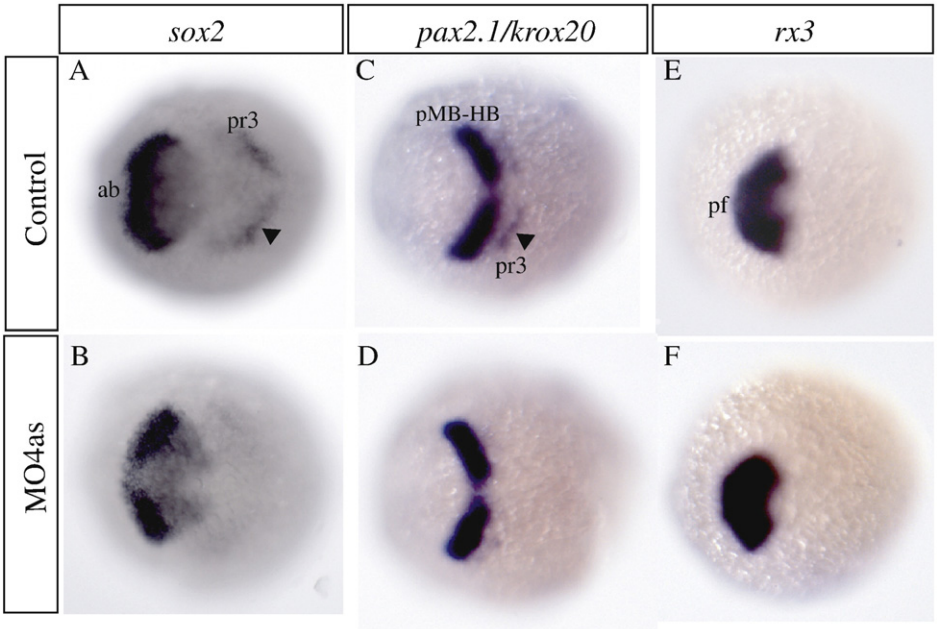


**Fig. 2.** *irx4a* regulates sox2 expression in the neural plate. *In situ* hybridization of brain markers was carried out on control and *irx4a* morphant embryos at 90% epiboly. (A, B) The neural precursor marker *sox2* appears diminished in the anterior brain (ab) and hindbrain (presumptive rhombomere 3, arrowhead, pr3) in *irx4a* morphant embryos (B) compared to uninjected controls (A). (C, D) The expression pattern of *pax2.1* in the midbrain–hindbrain boundary (pMB-HB) appears unaffected but the expression of the rhombomere 3 marker *krox20* (arrowhead) is diminished in morphant embryos. (E, F) *rx3* expression in the presumptive forebrain (pf) is unchanged in morphant compared to control embryos. All views are dorsal, anterior is towards the left.

placodes. Antisense knockdown of this gene in early zebrafish embryos reveals a function for *irx4a* in development of the trigeminal, anterior and posterior lateral line, otic and epibranchial placodes. In addition, we also demonstrate that *irx4a* participates in the formation of the retina and we show an evolutionary conservation in the function of this gene in heart chamber specification.

## Results

### *Loss-of-function of irx4a causes increased cell death in the brain but does not affect regional specification*

Expression of zebrafish *irx4a* mRNA has been described previously (Lecaudey et al., 2005). Briefly, expression at 80% epiboly is detected in a large bilateral stripe covering the midbrain and hindbrain. Later, at the tailbud stage, this gene is activated in a more caudal domain corresponding to the prospective spinal cord. During neurulation, *irx4a* shows expression in the midbrain, in the hindbrain, with strong expression in rhombomeres 1 and 4 (r1 and r4), and weaker expression in the caudal hindbrain and spinal cord with a diminishing rostro-caudal gradient. At 24 hpf *irx4a* has strong expression in the statoacoustic ganglion and the heart (Lecaudey et al., 2005). We carried out *in situ* hybridization (ISH) to detect *irx4a* expression and we find essentially ubiquitous distribution of transcripts at the 70% epiboly stage, with a pattern that becomes refined during post-gastrula stages as described previously (see Supplementary Fig. S1 and not shown).

We sought to study the function of the *irx4a* in early development by loss-of-function analysis. To achieve this, we injected embryos with Morpholino antisense oligonucleotides complementary to either the 5′ region of the transcript containing the initial ATG or to the splice site spanning the junction of exon 2 and intron 2 of the *irx4a* gene (MO4a and MO4as, respectively). The use of two different morpholinos against the gene allowed us to demonstrate a specific effect by comparing phenotypes obtained by knockdown of *irx4a* function. We did not notice significant differences between them and for the remaining experiments shown, we used MO4as. To corroborate the effect of MO4as on splicing, we carried out PCR using primers flanking the splicing site and find a complete absence of the processed mRNA band in morphant embryos (Fig. 1G). Control embryos were injected with 5 nl of a 1 μg/μl morpholino directed against the *zash1a* gene, which produces no overt phenotype (Sarrazin et al., 2006). At 24 hpf, live *irx4a* morphant embryos show a slight decrease in the overall size of the anterior brain and the eye (Figs. 1A, B, arrow), but the hindbrain, trunk and tail are of normal appearance. Later, at 48 hpf, they develop a prominent pericardial edema (data not shown) and die around 5 dpf. Analysis of cell death by incorporation of acridine orange and of proliferation by immunohistochemistry against phosphorylated Histone H3 (H3-P) show that the reduction in head size of morphants is more likely due to an increase in cell death than to a decrease in proliferation (Figs. 1C–F). To analyze whether there were patterning defects in the brain, we performed *in situ* hybridization analysis on wild type and morphant embryos at two different developmental stages using different brain markers: *sox2* (neural progenitors of the anterior brain; Okuda et al., 2006), *emx* and *rx3* (forebrain), *pax2.1* and *fgf8* (midbrain–hindbrain boundary) and *krox20* (hindbrain) (Fig. 2). At 10 hpf we observed diminished expression of the progenitor cell marker *sox2*, both in the forebrain and in presumptive rhombomere 3 (compare Figs. 2A and B). Expression of *krox20* in rhombomere 3 at this stage was also strongly diminished at this stage (Figs. 2C, D). Despite the loss of *sox2* expression in the forebrain in *irx4a* morphants (Fig. 2B), the anterior brain is correctly specified, as expression of *rx3* is not affected (Figs. 2E, F). We next analyzed expression of antero-posterior (A/P) patterning markers at 24 hpf. The injection of either morpholino produced no significant effect on the expression of any of the tested markers, indicating that overall anterior–posterior patterning of the neural tube, as well as establishment of the midbrain–hindbrain boundary is not perturbed (Figs. 3A–D). However, the reduction in the size of the brain did make the labeled regions appear more compact. Likewise, the expression pattern of two additional genes, *shh* and *c-myc*, was not

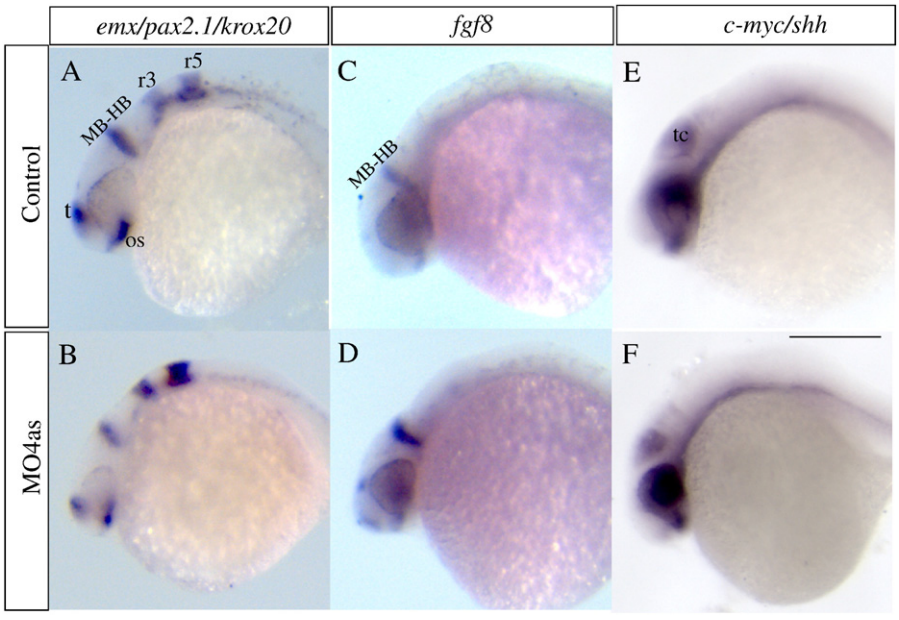


**Fig. 3.** *irx4a* inhibition does not significantly alter A/P or D/V patterning. *In situ* hybridization was carried out on 24 hpf embryos using CNS markers to evaluate potential patterning defects induced by inhibition of *irx4a* function. (A, B) At 24 hpf the expression patterns of the forebrain marker *emx*, the midbrain–hindbrain boundary marker *pax2.1* and the hindbrain marker *krox20* appear unaffected in morphant embryos compared to controls. (C, D) Expression of *fgf8* corroborates that the midbrain–hindbrain boundary is correctly established in morphant embryos. (E, F) Expression of *shh* and *c-myc* is unchanged in morphant embryos indicating that dorso-ventral patterning is also normally established in the absence of *irx4a* function. MB-HB, midbrain–hindbrain boundary; os, optic stalk; r3, rhombomere 3; r5, rhombomere 5; t, telencephalon; tc, tectum. The panel shows lateral views; dorsal is up, anterior is towards the left. Scale bar in (F) 50 μm.

altered, demonstrating that dorso-ventral (D/V) patterning is similarly unaffected by *irx4a* loss-of-function (Figs. 3E, F).

*irx4a is involved in hindbrain placodal specification*

Previous studies carried out in *Xenopus* and zebrafish have demonstrated a role for *Irx* genes in placodal specification (Itoh et al., 2002; Glavic et al., 2004). *Irx* genes are presumed to be involved in development of the posterior placodes, including the trigeminal, otic, lateral line and epibranchials (Schlosser, 2005 and 2006). We first used the earliest markers known to label the entire pre-placodal field, *eya1* and *six4.1*, at 90% epiboly and tailbud stage, and compared their expression in wild type and *irx4a* morphant embryos. Injection of 10 ng MO4as leads to a loss of the caudal-most expression domain of both *eya1* and *six4.1* (Figs. 4A–D). The neurogenic placodes express the proneural transcription factor *neurogenin1* (*ngn1*) beginning at the tailbud stage and expression continues during formation of the cranial ganglia. Examination of the expression pattern of *ngn1* in MO4as injected embryos revealed a decrease in the label in the trigeminal placode at 9 hpf (Figs. 4E, F) and a complete loss of its expression in the developing cranial ganglia at 18 hpf (Figs. 4G, H). This is similar to previous findings that showed that both *irx1b* and *irx7* regulate the expression of *ngn1* in the trigeminal ganglion (Itoh et al., 2002). The *neuroD* gene is regulated by *ngn1* and can be detected in the statoacoustic and lateral line ganglia at 24 hpf. At this stage we compared the expression of *neuroD* in uninjected and *irx4a* morphants by *in situ* hybridization. Morphant embryos show a strong reduction in the label in these ganglia compared to wild type embryos at this stage (Figs. 4I, J).

The neural crest and placodes develop similarly in several respects; both give rise to multiple non-epidermal cell types including neurons, glia, and secretory cells. Given the effects of *irx4a* inhibition on placodal development, we decided to analyze a neural crest marker in morphant embryos. We examined the expression pattern of the neural crest marker *foxd3* as well as GFP expression in *foxd3-GFP* transgenic embryos injected with *irx4a* morpholinos at 24 hpf and 48 hpf, respectively. We did not detect any differences between morphants and controls with these markers (Supplementary Fig. S2) suggesting that *irx4a* is not involved in neural crest development.

Taken together, these results indicate that *irx4a* has a fundamental function in the early specification of the posterior placodal field (caudal territories of *six4.1* and *eya1* expression) and that the absence of this gene disrupts the expression of genes that label at least a subset of the placodal derivates (*ngn1*, *neuroD*).

We next investigated whether the alteration in the specification of the posterior preplacodal field after *irx4a* knockdown affected development of specific placodes and their derivatives. To examine the otic placode, we analyzed the expression pattern of the *pax8* gene at 10 hpf. We found that morphant embryos showed moderately diminished expression of pax8 compared to wild type embryos (Figs. 5A, B). Later in development, the otic placode invaginates to form the otic vesicle, which gives rise to the inner ear and to neural precursors, which migrate away from the epithelium of the otic vesicle and form the sensory neurons of the statoacoustic ganglion (Fritzsch et al., 2002; Riley and Phillips, 2003; Barald and Kelley, 2004). We found that the territory that gives rise to the statoacoustic ganglion, labeled with the *irx1b* marker, is reduced as well in morphants (Figs. 5C, D) and is occasionally completely absent (not shown). Later in development however, the inner ear appears to form normally in morphants, as expression of GFP in a transgenic line that labels inner ear hair cells (SqET4, Parinov et al., 2004) is indistinguishable from control embryos (Figs. 5E, F). The caudal preplacodal field also gives rise to the epibranchial placodes and their derivatives, the geniculate, petrosal and nodose ganglia (Sahly et al., 1999; Zou et al., 2004). We examined these ganglia in control and morphant embryos using the *neuroD* probe and find that the label in the geniculate and nodose ganglia is absent in morphants at 72 hpf (Figs. 5G, H).

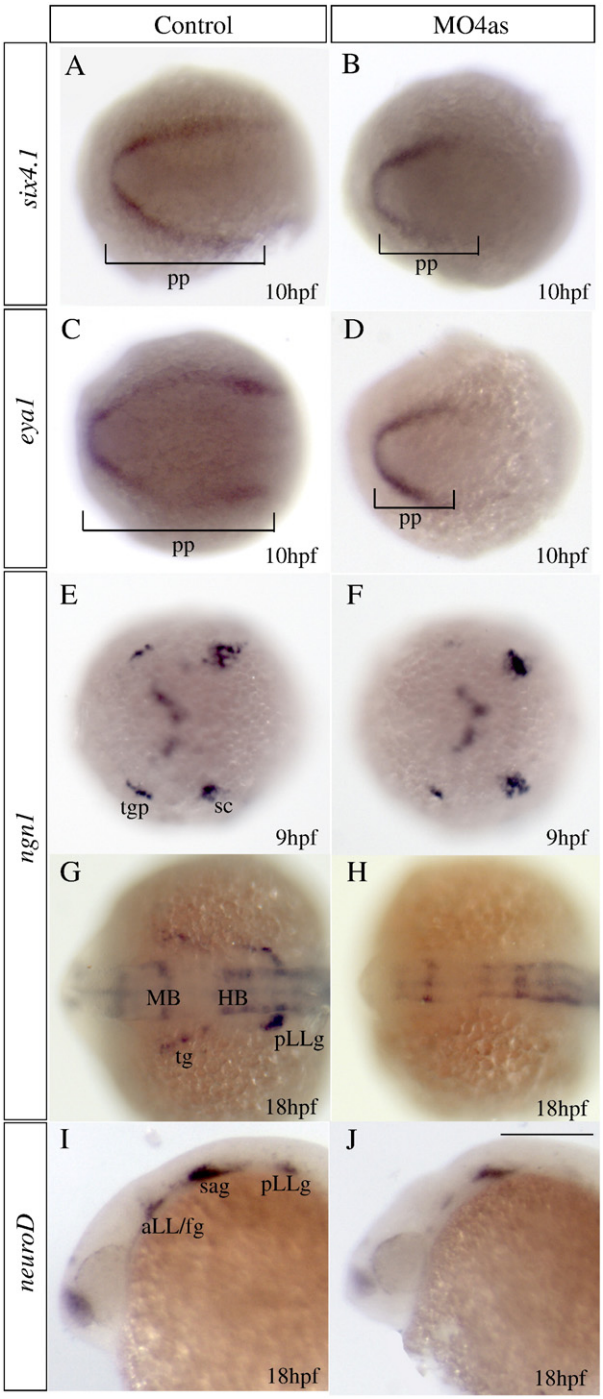


**Fig. 4.** *irx4a* is involved in specification of a subset of placodes. *In situ* hybridization results of embryos processed for detecting expression of the indicated marker genes. Embryos were fixed at 10 hpf (A–F), 17 hpf (G–H) or 24 hpf (I–J). (A–D) Injection of MO4as leads to an inhibition of the posterior expression domain of the preplacodal markers *six4.1* (compare A and B) and *eya1* (compare C and D). (E–H) *ngn1* expression is strongly diminished at 9 hpf in the trigeminal ganglion (tg) but not in the posterior lateral line ganglion (pLLg) in morphants (compare E to F). Later in development, at 17 hpf, expression of this marker is absent in the tg and pLLg (compare G to H). Expression of the proneural gene *neuroD* in the anterior and posterior lateral line ganglia is also affected in morphants (compare I to J). pp, preplacodal region; aLL, anterior lateral line placode; HB, hindbrain; MB, midbrain; sc, dorsal/lateral spinal cord; sa, statoacoustic ganglion; pLL, posterior lateral line placode; pLLg, posterior lateral line ganglion; tgp, trigeminal ganglion placode; tg, trigeminal ganglion. A–H are dorsal views; I, J show lateral views; anterior is towards the left. Scale bar in J: 40 μm for G–J.

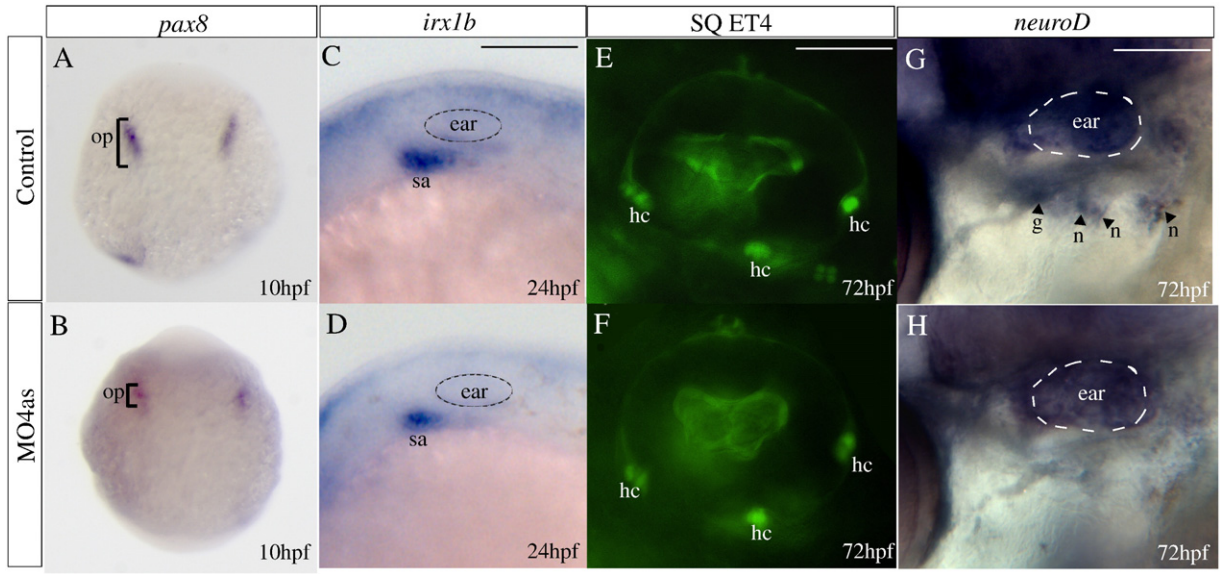


**Fig. 5.** Requirement of *irx4a* for epibranchial ganglia but not ear development. *In situ* hybridization results (A–D, G–H) and images of GFP expression in transgenic larvae (E–F) for control and *irx4a* morphant fish. (A, B) Expression of the otic placode marker *pax8* is slightly decreased in *irx4a* morphant embryos at 10 hpf. (C, D) Expression of the statoacoustic ganglion marker *irx1b* is similarly affected at 24 hpf. (E, F) Examination of hair cells (hc) in control and morphant SqET4 transgenic larvae shows no effect of the morpholino injection at 72 hpf. In this transgenic line, the three patches of hair cells in the ear can be observed in live fish. (G–H) *In situ* hybridization showing *neuroD* expression in the epibranchial ganglia (petrosal, p, and nodose, n) at 72 hpf. Note the absence of expression of this marker in morphant (H) compared to controls (G). hc, clusters of hair cells; n, nodose ganglia; sa, statoacoustic ganglion; o, otic placode; p, petrosal ganglion. A, B dorsal views of whole embryos. C–H lateral views centered on the otic vesicle. Scale bar in C: 15 μm for C, D; scale bar in E: 5 μm for E, F; scale bar in I: 10 μm for G, H.

*irx4a regulates the number of neurons in the trigeminal ganglion*

Rostral to the otic and anterior lateral line placodes lies the trigeminal placode. We had detected a drastic decrease in the expression of *ngn1* in the trigeminal placode in MO4as morphant embryos (Figs. 4E–H). We therefore decided to investigate possible effects of *irx4a* inhibition on development of the trigeminal neurons. The sensory neurons in this ganglion were labeled with two antibodies at 24 hpf: anti-islet1, which labels cell nuclei, and anti-acetylated tubulin, that labels cell bodies and neural projections. Comparison of control and morphant embryos shows an important requirement of *irx4a* for specifying the size of the ganglion as both markers are decreased in morphants (Figs. 6A–D). Counting cell nuclei in anti-islet1 stained embryos shows that there is a statistically significant decrease in cell number in morphants compared to controls (Fig. 6I). Since this result suggests that *irx4a* is required for

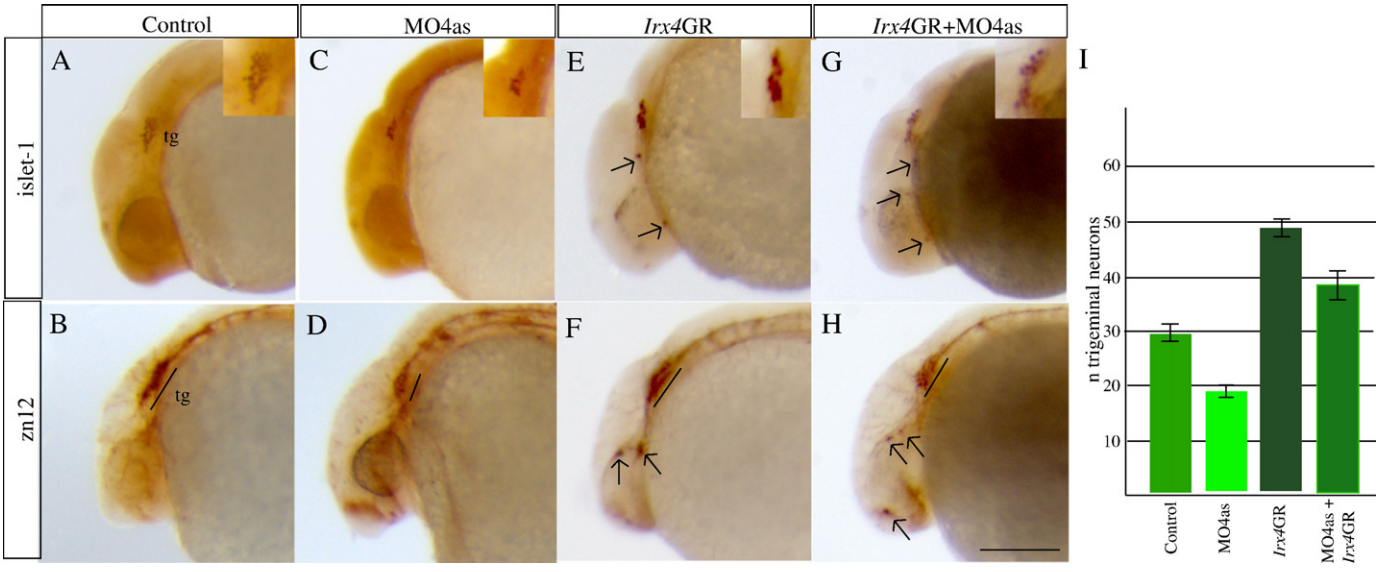


**Fig. 6.** *irx4a* regulates the number of neurons that form the trigeminal ganglion. *irx4a* morphant and control embryos were fixed at 24 hpf and processed for immunohistochemistry using the anti-Islet1 (A, C, E, G, insets show close-up images of the trigeminal area) or zn-12 antibodies (B, D, F, H). (A–D) Comparison of both antibody stains between control (A, B) and *irx4a* morphant (C, D) shows a drastic decrease in the number of neurons that form the trigeminal ganglion (compare A with C and B with D). (E, F) Gain of function experiments carried out by injection of *Irx4*GR mRNA show an increase in the number of trigeminal neurons (compare A with E and B with F) and occasional appearance of ectopic expression of both antibody markers in other areas of the head (arrows). (G, H) Coinjection of MO4as and *Irx4*GR mRNA recovers near-normal numbers of neurons in the trigeminal ganglion though there is remaining ectopic expression of Islet-1 and zn-12 antigen in the head. I, the number of anti-Islet1 labeled neurons in the trigeminal ganglia were counted in control, MO4as, *Irx4*GR and MO4as+*Irx4*GR embryos. An average for 30 embryos with S.D. was calculated. A–H show lateral views of the anterior region of embryos; dorsal is up, anterior is left. Scale bar in H: 40 μm.

specifying the correct number of trigeminal neurons, we next carried out a gain-of-function experiment with *irx4a*. Injection of *irx4a* mRNA produced pleiotropic effects in many regions of the embryo that lead to early lethality. Therefore, we decided to use an inducible system for overexpression of the gene. We took advantage of the availability of the *Xenopus Irx4GR* construct, which contains a fusion between the *Irx4* gene and the glucocorticoid receptor, making it temporally inducible by addition of dexamethasone to the culture medium (De Graaf et al., 1998). We injected *Irx4GR* mRNA into one-cell stage embryos, added dexamethasone to the growth medium at 10 hpf to activate the protein, and analyzed the effects on trigeminal ganglion development as before. We detected a significant increase in both the size (anti-acetylated tubulin) and number of cell nuclei (anti-islet1) in trigeminal ganglia of induced embryos compared to uninduced injected controls (Figs. 6E, F and I). We often detected the production of ectopic trigeminal neurons in other areas of the head (Figs. 6E and F, arrows), suggesting that activation of this gene in other placodal regions may be sufficient to elicit a fate change towards trigeminal ganglion sensory neurons. Since we observed loss of trigeminal neurons using the *irx4a* morpholino, we attempted to rescue the phenotype with expression of the inducible *Irx4* gene, which, on its own, produces the opposite effect. Co-injection of both reagents, and induction of Irx4GR at 10 hpf, produced embryos that recovered nearly normal numbers of trigeminal neurons (Fig. 6I), though there were still occasional ectopic islet/acetylated tubulin-labeled neurons in regions distant from the trigeminal area (Figs. 6G, H). It must be noted that the morpholino directed against the zebrafish *irx4a* gene will not interfere with expression of *Xenopus Irx4* as there is no sequence complementarity between the morpholino and the frog gene.

### *irx4a function in lateral line development*

The anterior and posterior lateral line placodes give rise to all peripheral components of the lateral line system, a sensory complex used for detection of water movements and electric fields that is

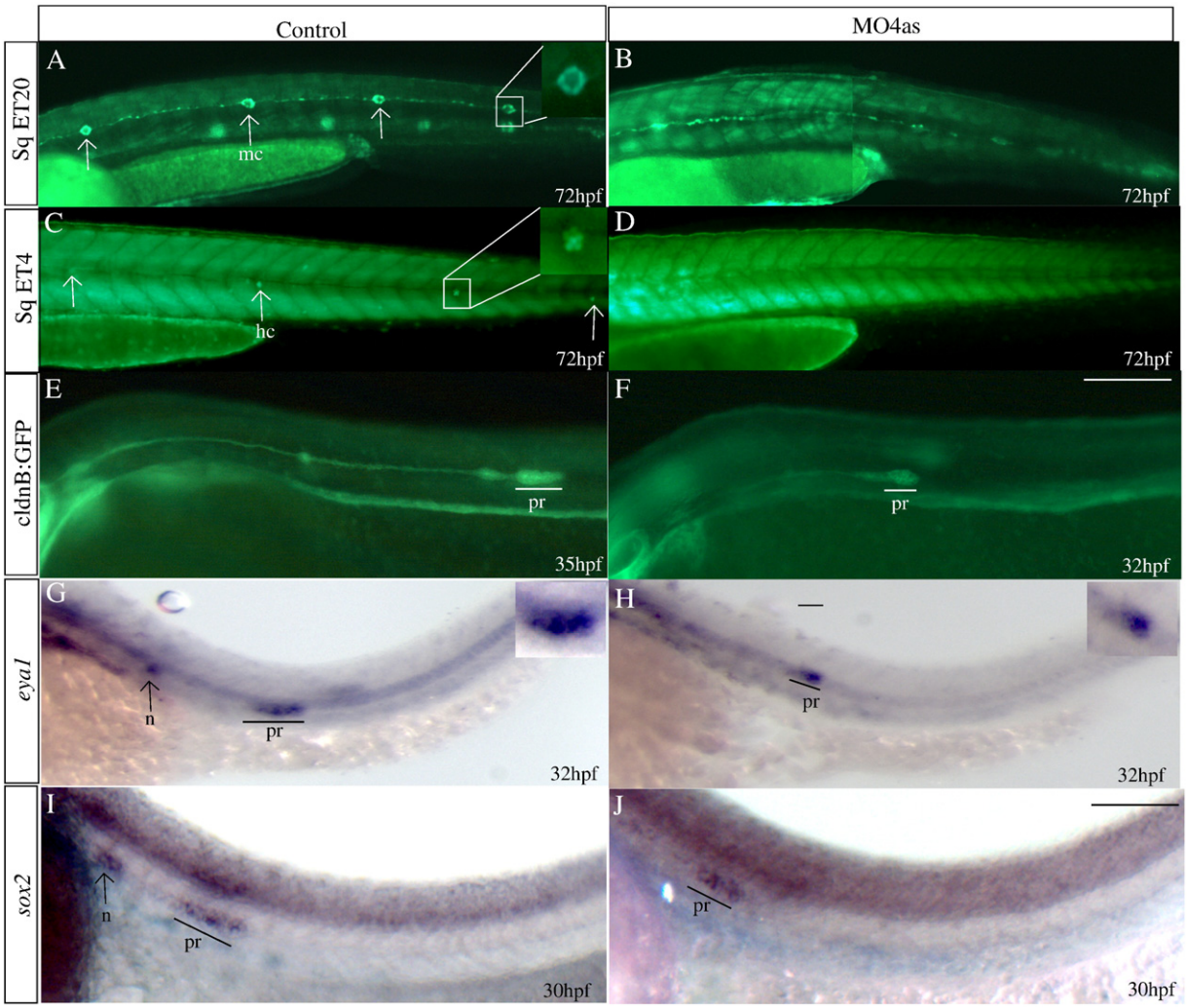


**Fig. 7.** *irx4a* is required for the correct development of the posterior lateral line. GFP expression was observed in the SqET20 (A, B), SqET4 (C, D) and cldnB:GFP (E, F) transgenic lines in control and morphant larvae at the indicated times post-fertilization. *In situ* hybridization was carried out using the *eya1* (G, H) and *sox2* (I, J) riboprobes. (A, B) Expression of GFP in 72 hpf control SqET20 transgenic line labels mantle cells (arrows in A, inset) and interneuromastic cells (inc). Morphant embryos (B) lack neuromast mantle cells but interneuromastic cells are present indicating that primordium migration occurred. (C, D) At 72 hpf mechanosensory hair cells (arrows in C, inset) are labeled in the SqET4 transgenic line while morpholino injected siblings (D) show the absence of these cells. (E, F) The migrating primordium, the trail of interneuromastic cells and deposited neuromasts express GFP in cldnB:GFP transgenic uninjected embryos (E). In contrast, MO4as injected cldnB:GFP embryos (F) show a decrease in the size of the migrating primordium and the absence of deposited neuromasts. Note that we have compared GFP label in a 32 hpf morphant with a 35 hpf control embryo. The primordium size difference is evident despite the fact that the primordium in the control fish has already deposited two neuromasts. (G–J) Expression of the primordium markers *eya1* (G, H, insets show magnified views) and *sox2* (I, J) shows a similar effect, the label is diminished in morphant embryos. inc, interneuromastic cells hc, hair cells; n, neuromast; pr, primordium. The entire panel shows lateral views of the trunk and tail region; dorsal is towards top, anterior is towards left. Scale bar in F: 50 μm for A–F, scale bar in J: 30 μm for G–J.

present only in fish and aquatic amphibians (Ghysen and Dambly-Chaudiere, 2004). The individual sensory organs are named neuromasts and they are organized in species-specific patterns in the ectoderm of the head and along the trunk and tail. In zebrafish, the neuromasts (formed by hair cells, accessory cells and innervated by lateral line ganglion neurons) are deposited at stereotyped locations in the body by migrating primordia, groups of cells that delaminate from the respective placodes and move cohesively over the body surface during late embryogenesis (Ghysen and Dambly-Chaudiere, 2004; Gibbs, 2004; Schlosser, 2006). We had observed loss of expression of *ngn1* and *neuroD* in *irx4a* morphant embryos, two proneural genes expressed in the lateral line placodes and derivatives (Andermann et al., 2002; Sarrazin et al., 2006). To investigate whether *irx4a* is involved in the development of the lateral line system, we analyzed posterior lateral line primordium migration and neuromast deposition in morphants using the transgenic lines SqET20 (that expresses GFP in the migrating primordium and in a group of accessory cells, the mantle cells, Fig. 7A) and SqET4 (that expresses GFP in hair cells, Fig. 7C) (Parinov et al., 2004). The analysis of *irx4a* morphant SqET20 transgenic embryos indicates that the primordium migrates correctly, as these cells can be seen during migration (not shown) and because of the presence of a trail of interneuromastic cells, normally left behind by the primordium (Fig. 7B). However, there was no neuromast differentiation in morphant embryos as there are no detectable mantle cells (Fig. 7B) or hair cells (Fig. 7D) in the *irx4a* knockdown embryos. To examine the size and structure of the primordium more closely, we first used an additional transgenic line, claudinB:GFP (Hass and Gilmour, 2006), that labels these cells. While it is apparent that the primordium migrates in morphant embryos, its size is smaller than that of controls, even though it does not lose cells due to neuromast deposition along its migratory path as wild type primordia do (Figs. 7E, F). Secondly, we analyzed the expression of two genes that label the migrating primordium in morphant and control embryos: *eya1* (Sahly et al., 1999) and *sox2* (Hernández et al., 2007). Both of these probes showed decreased labeling in *irx4a* morphants (Figs. 7G–J). These results suggest that the failure in neuromast deposition in morphant embryos could be due to a reduction in the number of cells in the posterior lateral line placode, which gives rise to the migrating primordium.

### *Conserved function of irx4a in heart and eye development*

The vertebrate heart consists of two types of chambers, the atria and the ventricles, which differ in their contractile and electrophysiological properties. In chick, expression of *irx4* is restricted to the ventricle at all stages of heart development and regulates the chamber specific expression of myosin isoforms by activating the expression of the ventricle myosin heavy chain (*vmhc1*) and suppressing the expression of the atrial myosin heavy chain (*amhc1*) (Bao et al., 1999). Expression of *irx4* in the heart is highly conserved in evolution, as it is also expressed in this tissue in mouse, *Xenopus* and zebrafish (Chistoffetls et al., 2000, Garriock et al., 2001; Lecaudey et al., 2005). To explore a possible role for *irx4a* in heart development, we injected embryos with MO4as or control morpholino, fixed at 24 hpf and 36 hpf, and analyzed the formation of the atrium and ventricle by *in situ* hybridization using the specific markers *amhc1* and *vmhc1*. In morphant embryos, we detected an increase in the size of the atrium marker (Figs. 8A, B) simultaneous with a decrease in expression of the ventricle marker (Figs. 8C, D). We conclude that the function of the *irx4a* in cardiac chamber specification is likely to be conserved from fish to mammals.

A second conserved function of the *Irx* family of genes is their participation in eye development. In *Drosophila*, *iroquois* genes are required for the patterning of the dorsoventral axis of the eye imaginal discs (McNeill et al., 1997; Dominguez and de Celis, 1998; Cavodeassi et al., 1999). In the chick retina, *irx4* has been related with axon pathfinding (Jin et al., 2003), while in the mouse, all six *Irx* genes are expressed in the developing retina (Cohen et al., 2000; Bosse et al., 2000; Houweling et al., 2001). Furthermore, zebrafish *irx1a* has been implicated in retinogenesis (Cheng et al., 2006). We examined the structure of the embryonic retina in *irx4a* morphant embryos by monitoring HNK-1 expression using the Zn12 antibody, which labels retinal ganglion cells beginning at 48 hpf (Hu and Easter, 1999). We find that in 72 hpf morphant embryos Zn-12 label is undetectable in

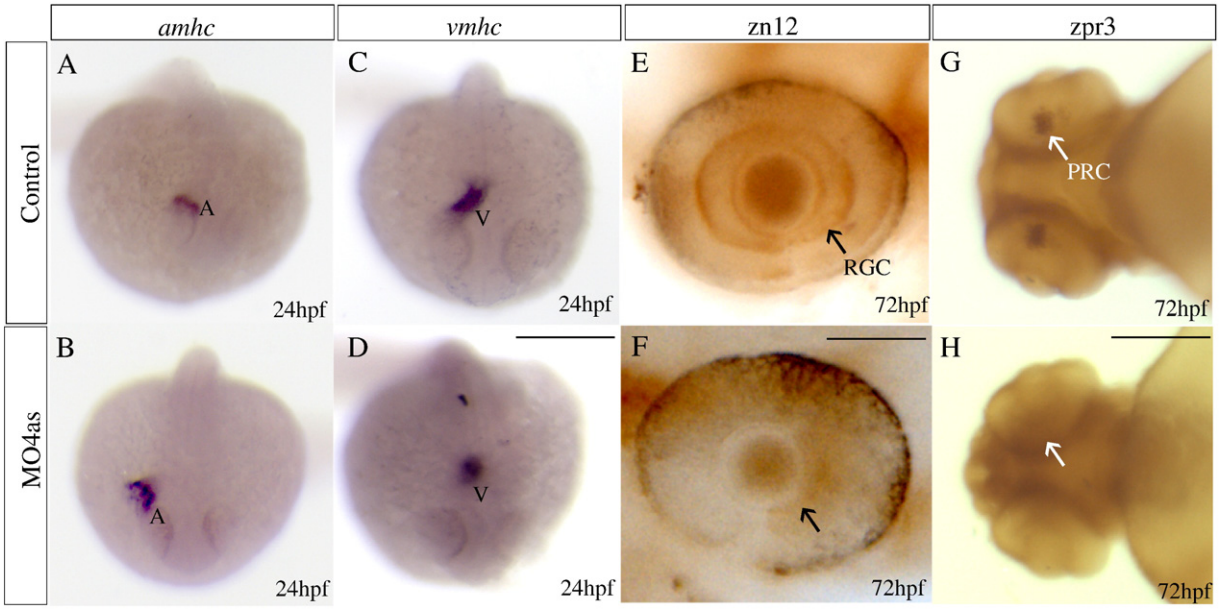


**Fig. 8.** *irx4a* is involved in cardiac chamber specification and retinal development. Control and *irx4a* morphant embryos were processed for *in situ* hybridization (A–D) or immunohistochemistry (E–H). (A–D) Morphant embryos (B, D) show an increase in the size of the atrium and a decrease in the size of the ventricle compared to control embryos (A, C) as revealed the expression of the *amhc* (A, B) and *vmhc* (C, D) markers, respectively. (E, F) zn12 immunostaining labels retinal ganglion cells (RGC) in control embryos (E, arrow) but they are not detected in MO4as injected embryos (F). (G, H) zpr-3 immunostaining labels photoreceptor cells (PRC) in the 72 hpf control larva (G, arrow) but not in the morphant larva (H); note that photoreceptors have only differentiated in the ventral retina at this stage. A–D, dorsal views of whole embryos at 24 hpf, anterior is down; E, F, lateral views of the eye at 72 hpf, anterior is left; G, H, ventral views of the head. Scale bar in D: 40 μm for A–D, scale bar in F: 7 μm for E, F; scale bar in H: 15 μm for G, H.

the retina (Figs. 8E, F). Similarly, antibody labeling using zpr-3, that labels cones in the photoreceptor cell layer, also indicates that this cell type is absent in morphant embryos (Figs. 8G, H). These results suggest that neurogenesis in the retina and formation of two important cell types requires *irx4a*.

## Discussion

Our results indicate that the zebrafish *irx4a* gene participates in development of several tissues, including the eye and heart as has been reported in other organisms. However, here we describe a role for *irx4a* in sensory placode development, a function previously described for other members of this family but not for *irx4* genes. Moreover, elucidation of *Irx* gene function in placodes and derivatives has been shown until now either using dominant negative constructs, that often show pleiotropic effects, or using multiple morpholinos, as was the case with *irx7* and *irx1* in zebrafish (Itoh et al., 2002). This is the first example of a function assigned unambiguously to a single *Irx* gene in vertebrate placode development. Expression of *irx4a* early in embryogenesis is restricted to wide domains in the CNS and later becomes restricted to specific regions such as the midbrain, hindbrain and spinal cord (Lecaudey et al., 2005). While these authors do not report expression in sensory placodes, the early expression in domains that extend laterally beyond the edges of the neural plate is consistent with an early role in placode formation. We also see widespread expression of this gene in mid gastrulation (70% epiboly) and we cannot exclude that low levels of transcripts remain in additional tissues throughout development. Moreover, Lecaudey et al. (2005) report expression in cranial ganglia (gVIII) after 24 hpf.

In our study, we inhibited translation and/or splicing of *irx4a* transcripts by using specific antisense morpholinos. While most of the expression of this gene is confined to the neural plate and, later, the neural tube, perturbing the function of *irx4a* does not appear to cause widespread CNS patterning defects, as the specific markers used to examine brain regionalization appeared unaffected, at least until the 24 hpf stage. By this stage though, morphant embryos appear to have slightly smaller heads and eyes compared to controls. We detected extensive cell death in the CNS of morphants indicating that *irx4a* is required for cell survival in anterior structures. Our analysis of the neural progenitor cell marker *sox2* (Okuda et al., 2006) at 10 hpf showed differences in expression levels between morphant and control embryos in the anterior neural plate and presumptive hindbrain. Sox2 is required for maintenance of neural progenitor cells in the nervous system and partial loss of this gene's activity could account for the observed cell death phenotype and the size difference with wild type embryos. We conclude that either this change in sox2 expression does not alter patterning of the different brain regions or, alternatively, that the perturbations are rescued by 24 hpf. Our results also suggest that *sox2* may be a direct target of *irx4a*, as has been demonstrated in *Xenopus* for *Irx1* (Glavic et al., 2004). The relatively minor effect of diminished *sox2* expression could be due to redundancy among *SoxB1* family members as they show extensive overlap in expression domains (Okuda et al., 2006). Moreover, loss of *sox2* function in zebrafish produces no overt phenotype in the CNS (our unpublished results).

Development of retinal ganglion cells and photoreceptors in the retina is impaired by abrogation of zebrafish *irx4a*. This result suggests that *irx4a* could be playing a role in early neurogenesis but exactly how this role is fulfilled remains to be determined. In *Drosophila*, *Iroquois* genes directly regulate proneural genes, such as those of the *achaete-scute* family of transcription factors (Gómez-Skarmeta et al., 1996; Leyns et al., 1996). Examination of such a relationship in vertebrate neurogenesis could provide insights as to the exact molecular function of *Irx* genes, including *irx4a* in the zebrafish retina.

Members of the *Irx* gene family have been shown to be critical for placode derivative development (Itoh et al., 2002; Glavic et al., 2004). We therefore examined the role of *irx4a* in early specification of the placodal territory and formation of placodal derivatives. In *irx4a* morphant embryos at 10 hpf we detected a strong reduction in the posterior expression domain of two panplacodal markers, *eya1* and *six4.1*. This region gives rise to posterior ganglia including the trigeminal, epibranchial, lateral line and statoacoustic ganglia, as well as the otic vesicle. When we examined markers for specific cranial placode derivatives at 24 hpf or later, the absence of *irx4a* function results in a very clear loss of a subset of the labeled ganglia derived from these placodes. Expression of *ngn1* in the trigeminal ganglion is diminished at 10 hpf and is undetectable in morphants by 18 hpf. There is prior evidence showing that *ngn1* is a target of *irx1b*/*irx7* in the trigeminal ganglion and that these members of the *Irx* family are crucial for trigeminal neuron formation (Itoh et al., 2002). Similarly, *neuroD* is strongly reduced in the trigeminal, epibranchial and lateral line ganglia at later stages in *irx4a* morphant embryos. This is consistent with previous reports that suggest that *NeuroD* is a direct target of *ngn1* in cranial ganglia (Andermann et al., 2002). We found a modest reduction in the expression levels of *pax8*, an otic placode marker in *irx4a* morphants. However, formation of the otic vesicle was not affected under this condition, as sensory cells differentiated normally.

We examined the differentiated ganglia to determine whether the loss of early markers was accompanied by loss of neurons. The trigeminal and epibranchial neurons appeared less numerous in morphants compared to uninjected siblings. In the case of the trigeminal sensory neurons, we were able to count the number of cells in each case using and anti-islet1 antibody: loss of *irx4a* reduced the number of neurons in this ganglion by about 40%. Interestingly, we obtained the opposite effect when we overexpressed the *Xenopus irx4* gene (*Irx4*) in zebrafish embryos: in this case we observed an increase of approximately 40% in the number of trigeminal neurons. While we cannot exclude the possibility that overexpression of *Irx4* has non-specific effects or activates targets of other *Irx* family members, we were able to revert to nearly normal numbers of trigeminal neurons by co-injecting the mRNA and the morpholino. The overexpression experiment also revealed ectopic formation of trigeminal neurons in different regions of the head ectoderm as detected with two different markers. However, we cannot attribute a role for *Irx4* (or *irx4a*) in controlling trigeminal neuron identity. The presence of a highly conserved homeodomain in the expressed protein is likely to allow promiscuous binding to targets of other Irx family members. Nonetheless, the combination of our results does imply that *irx4a* has a role in determining the number of neurons in the trigeminal ganglion.

We observed a similar function for *irx4a* in development of the lateral line. In this case, we examined a derivative of the posterior lateral line placode, the posterior migrating primordium, which forms the posterior primary neuromasts. Two markers for these cells, *eya1* and *sox2*, showed diminished expression in *irx4a* morphants, and live images of GFP-expressing primordium cells in morpholino injected transgenic larvae showed less cells than their uninjected siblings. The outcome resulting from this cell loss was a failure in deposition of neuromasts, and therefore, the absence of differentiated lateral line sensory and accessory cells. Sox2 labels progenitors in the primordium and neuromasts and is likely to be critical for development of the lateral line as it is for the sensory component of the inner ear (Kiernan et al., 2005; Hernández et al., 2007). As we saw a regulatory relationship between *irx4a* and *sox2* in the neural plate, this could also be the case in the lateral line system, where *sox2* is expressed (Hernández et al., 2007). Diminished *sox2* expression could lead to a reduction in the number of progenitors in *irx4a* morphant embryos and this in turn may lead to a loss of neurogenic potential in the lateral line system. Once again, we uncover the possibility that *irx4a* is regulating *sox2* expression in this territory; however, further evidence will have to be obtained for this relationship to be confirmed.

Finally, we have shown that two known functions for *Irx4* genes in other species are conserved in the zebrafish. Specification of the heart chambers by *Irx4* has been shown in the chick, and we provide evidence that this occurs in fish as well. Likewise, the absence of *irx4a* function in zebrafish precluded the differentiation of retinal cells, which correlates with data from chick, mouse and amphibians that links this *Irx* family member with retinal development (Dominguez and de Celis, 1998; Cavodeassi et al., 1999; Jin et al., 2003; Cohen et al., 2000; Bosse et al., 2000; Houweling et al., 2001; Cheng et al., 2006). It remains to be seen whether the role for this gene in placode development is conserved across vertebrates as well.

## Experimental methods

### *Zebrafish lines and imaging*

Wild type fish were raised in our facility according to standard protocols (Westerfield, 1994). Embryos were raised at 28 °C in E3 medium (5 mM NaCl, 0.17 mM KCl, 0.33 mM $CaCl_2$, 0.3 mM $MgSO_4$, 0.1% Methylene Blue) and, when necessary, were anesthetized and fixed in 4% paraformaldehyde overnight at 4 °C. Developmental timepoints are expressed as hours post-fertilization (hpf). The SqET4 line expresses GFP in hair cells in the ear and the SqET20 in the neuromast mantel cells (Parinov et al., 2004); both lines were a kind gift of Vladimir Korzh. Photographs were taken in a Leica MZ12 dissecting microscope with a Leica DFC 300FX camera. Images were processed with Photoshop 7.0 for Macintosh. For all of the experiments described, the images shown are representative of the effects observed when these were present in more than 70% of the individuals (minimum of 50 embryos per experiment). All experiments were repeated at least three times.

### *Whole mount in situ hybridization and immunohistochemistry*

*In situ* hybridization was done as previously described (Jowett and Lettice, 1994). The following genes were obtained as cDNA clones and were used as templates for making RNA probes: *irx4a* (Genbank ID BC065966), *neuroD* (Blader et al., 1997 and Korzh et al., 1998), *shh* (Krauss et al., 1993), *c-myc* (Schreiber-Agus et al., 1993), *vmhc*, *amhc* (Berdougo et al., 2003), *fgf8* (Fürthauer et al. 1997), *emx* (Morita et al., 1995), *krox20* (Woo and Fraser, 1998), *ngn1* (Blader et al., 1997, Kim et al., 1997), *sox2* (Hernandez et al., 2007), *eya1* (Sahly et al., 1999), *pax8* (Lun and Brand, 1998), *irx1b* (Wang et al., 2001), *six4.1* (Seo et al., 1998) and *pax2.1* (Pfeffer et al., 1998). For immunohistochemistry, the following antibodies were used: mouse anti-acetylated tubulin (Sigma T6793); mouse Islet-1 (Developmental Studies Hybridoma Bank); mouse anti HNK-1/zn12 and zpr-3 (purchased from ZIRC, http://zebrafish.org; Trevarrow et al., 1990); rabbit Anti-phospho-Histone H3 (H3-P, Upstate 07-424), rabbit anti-GFP (Molecular Probes A11122). Immunolabeling was carried out essentially as described in Sarrazin et al. (2006).

### *Irx4GR construct*

We first generated a fusion construct containing the *Xenopus Irx4* cDNA and a *myc* tag, a construct called *Irx4*-MT. A DNA fragment from the 3′ region of the *Irx4* cDNA, which includes a unique KpnI site within the ORF, was PCR-amplified with the following primers: (5′-CCATGGTACCTACCCTCG-3′) and (5′-CCAATCGATAGCAAGATG-TTCTGTTCCT-3′). A ClaI site was included in the 3′ primer. The PCR fragment was cloned in the pGEM-T Easy vector and sequenced. Next, a ClaI/KpnI fragment containing the 5′ cDNA was ligated with the KpnI/ClaI 3′ cDNA into the ClaI site of pCS2-MT. We next cloned the GR domain between XhoI and XbaI, located 3′ of the Irx4-MT, into the pCS2 *Irx4*-MT vector. The hormone-inducible GR domain was obtained by PCR using the oligonucleotides (5′-cccctcgagATCCCC-TCTGAAAATCC-3′) and (5′-ctctagaCACTTTTGATGAAACAGAAG-3′) from a MyoD-GR plasmid kindly donated by H. Sive.

### *RNA and morpholino (MO) injection*

Two *irx4a* morpholinos were designed to knockdown translation of the Irx4a protein. MO4a was directed against the translation initiation region of the mRNA (5′-TCCGAATTGAGGATAGGACATTGTA-3′) while MO4as was designed to bind to the donor splice site between exon 2 and intron 2 (5′-CAATCTGAGCATCTTACCTGAGGTG-3′). Both were injected at a concentration of 1 μg/μl into one-cell stage embryos. To evaluate the inhibition of MO4as on *irx4a* mRNA splicing, we designed primers spanning the junction between exon 2 and intron 2. A band of 330 bp should be produced only if the morpholino inhibits correct removal of intron 2. For RT-PCR total RNA was extracted from 24 hpf morphants and control embryos and amplification was carried out for 30 cycles. Primers used for RT-PCR were Firx4a, 5′-CCGGCTGTTGGCCACCGCCAG-3′ and Rirx4a, 5′-GTCAGCCCAAACACC-GAAGAG-3′. Control primers amplify the βactin2 mRNA and were: F, 5′-TGTCTTCCCATCCATCGTG-3′ and R, 5′-AGGTCACGGCCAGCCAAG-3′. The *Irx4*GR construct was transcribed in vitro (digestion with NotI, transcription with Sp6) and mRNA was injected at 250 ng/μl in one-cell stage embryos. Translocation of the *Irx4*GR protein into the nucleus was induced by transferring embryos at the tailbud stage (10 hpf) into medium containing 10 mM Dexamethasone (Sigma D-4902) and incubating in this medium until fixed for analysis.

### *Acridine orange staining*

For characterization of cell death, embryos were stained according to Williams et al. (2000). Briefly, embryos were incubated for 20 min in 5 μg/ml Acridine Orange (Sigma) in embryo medium, washed three times for 5 min in embryo medium and observed under fluorescence microscopy.

## Acknowledgments

We thank Catalina Lafourcade and Florencio Espinoza for their technical help and Virginie Lecaudey and Sylvie Schneider-Maunoury for their helpful discussions. We also thank Deborah Yelon for her kind gift of probes. MA was supported by grants from Fondecyt (1070867), ICM (P06-039F), UNAB DI46-05R, and a CSIC-CONICYT exchange grant.

## Appendix A. Supplementary data

Supplementary data associated with this article can be found, in the online version, at doi:10.1016/j.mcn.2008.11.003.

## References

Andermann, P., Ungos, J., Raible, D.W., 2002. Neurogenin1 defines zebrafish cranial sensory ganglia precursors. Dev. Biol. 251, 45–58.

Bao, Z.Z., Bruneau, B.G., Seidman, J.G., Seidman, C.E., Cepko, C.L., 1999. Regulation of chamber-specific gene expression in the developing heart by Irx4. Science 283, 1161–1164.

Barald, K.F., Kelley, M.W., 2004. From placode to polarization: new tunes in inner ear development. Development 131, 4119–4130.

Bellefroid, E.J., Kobbe, A., Gruss, P., Pieler, T., Gurdon, J.B., Papalopulu, N., 1998. Xiro3 encodes a *Xenopus* homolog of the *Drosophila Iroquois* genes and functions in neural specification. EMBO J. 17, 191–203.

Berdougo, E., Coleman, H., Lee, D.H., Stainier, D.Y., Yelon, D., 2003. Mutation of weak atrium/atrial myosin heavy chain disrupts atrial function and influences ventricular morphogenesis in zebrafish. Development 130, 6121–6129.

Blader, P., Fischer, N., Gradwohl, G., Guillemot, F., Strahle, U., 1997. The activity of *neurogenin1* is controlled by local cues in the zebrafish embryo. Development 124, 4557–4569.

Bosse, A., Stoykova, A., Nieselt-Struwe, K., Chowdhury, K., Copeland, N., Jenkins, N.A., Gruss, P., 2000. Identification of a novel mouse *Iroquois* homeobox gene, *Irx5*, chromosomal localization of all members of the mouse *Iroquois* gene family. Dev. Dyn. 218, 160–174.

Brugmann, S.A., Pandur, P.D., Kenyon, K.L., Pignoni, F., Moody, S.A., 2004. Six1 promotes a placodal fate within the lateral neurogenic ectoderm by functioning as both a transcriptional activator and repressor. Development 131, 5871–5881.
Cavodeassi, F., Diez del Corral, R., Campuzano, S., Dominguez, M., 1999. Compartments and organising boundaries in the *Drosophila* eye: the role of the homeodomain Iroquois proteins. Development 126, 4833–4942.
Cavodeassi, F., Modolell, J., Gómez-Skarmeta, J.L., 2001. The *Iroquois* family of genes: from body building to neural patterning. Development 128, 2847–2855.
Cheng, C.W., Yan, C.H., Hui, C.C., Strahle, U., Cheng, S.H., 2006. The homeobox gene *irx1a* is required for the propagation of the neurogenic waves in the zebrafish retina. Mech. Dev. 123, 252–263.
Christoffels, V.M., Keijser, A.G., Houweling, A.C., Clout, D.E., Moorman, A.F., 2000. Patterning the embryonic heart: identification of five mouse Iroquois homeobox genes in the developing heart. Dev. Biol. 224, 263–274.
Cohen, D.R., Cheng, C.W., Cheng, S.H., Hui, C.C., 2000. Expression of two novel mouse Iroquois homeobox genes during neurogenesis. Mech. Dev. 91, 317–321.
De Graaf, M., Zivkovic, D., Joore, J., 1998. Hormone-inducible expression of secreted factors in zebrafish embryos. Dev. Growth Differ. 40, 577–582.
De la Calle-Mustienes, E., Feijóo, C.G., Manzanares, M., Tena, J.J., Rodríguez-Seguel, E., Letizia, A., Allende, M.L., Gómez-Skarmeta, J.L., 2005. A functional survey of the enhancer activity of conserved non-coding sequences from vertebrate Iroquois cluster gene deserts. Genome Res. 15, 1061–1072.
Dildrop, R., Ruther, U., 2004. Organization of *Iroquois* genes in fish. Dev. Genes Evol. 214, 267–276.
Domínguez, M., De Celis, J.F., 1998. A dorsal/ventral boundary established by Notch controls growth and polarity in the *Drosophila* eye. Nature 396, 276–278 200.
Feijoo, C.G., Manzanares, M., De la Calle-Mustienes, E., Gomez-Skarmeta, J.L., Allende, M.L., 2004. The *Irx* gene family in zebrafish: genomic structure, evolution and initial characterization of *irx5b*. Dev. Genes Evol. 214, 277–284.
Fritzsch, B., Beisel, K.W., Jones, K., Fariñas, I., Maklad, A., Lee, J., Reichardt, L.F., 2002. Development and evolution of inner ear sensory epithelia and their innervation. J. Neurobiol. 53, 143–156.
Fürthauer, M., Thies, C., Thies, B., 1997. A role for FGF-8 in the dorsoventral patterning of the zebrafish gastrula. Development 124, 4253–4264.
Garcia-Castro, M.I., Marcelle, C., Bronner-Fraser, M., 2002. Ectodermal Wnt function as a neural crest inducer. Science 297, 848–851.
Garriock, R.J., Vokes, S.A., Small, E.M., Larson, R., Krieg, P.A., 2001. Developmental expression of the *Xenopus Iroquois*-family homeobox genes, Irx4 and Irx5. Dev. Genes Evol. 211, 257–260.
Ghysen, A., Dambly-Chaudière, C., 2004. Development of the zebrafish lateral line. Curr. Opin. Neurobiol. 14, 67–73.
Glavic, A., Maris Honore, S., Feijoo, C.G., Bastidas, F., Allende, M.L., Mayor, R., 2004. Role of BMP signaling and homeoprotein Iroquois in the specification of the cranial placodal field. Dev. Biol. 272, 89–103.
Gomez-Skarmeta, J.L., Modolell, J., 1996. *araucan* and *caupolican* provide a link between compartment subdivisions and patterning of sensory organs and veins in the *Drosophila* wing. Genes Dev. 10, 2935–2945.
Gomez-Skarmeta, J.L., Modolell, J., 2002. *Iroquois* genes: genomic organization and function in vertebrate neural development. Curr. Opin. Genet. Dev. 12, 403–408.
Gómez-Skarmeta, J.L., Diez del Corral, R., de la Calle-Mustienes, E., Ferrés-Marcó, D., Modolell, J., 1996. araucan and caupolican, two members of the novel Iroquois complex, encode homeoproteins that control proneural and vein forming genes. Cell 85, 95–105.
Gomez-Skarmeta, J.L., Glavic, A., De la Calle-Mustienes, E., Modollel, J., Mayor, R., 1998. *Xiro*, a *Xenopus* homolog of the *Drosophila Iroquois* complex genes, controls development al the neural plate. EMBO J. 17, 181–190.
Gibbs, M.A., 2004. Lateral line receptors: where do they come from developmentally and where is our research going? Brain Behav. Evol. 64, 163–181.
Hass, P., Gilmour, D., 2006. Chemokine signaling mediates self-organizing tissue migration in the zebrafish lateral line. Dev. Cell 10, 673–680.
Hernandez, P.P., Olivari, F.A., Sarrazin, A.F., Sandoval, P.C., Allende, M.L., 2007. Regeneration in zebrafish lateral line neuromasts: expression of the neural progenitor cell marker *sox2* and proliferation-dependent and -independent mechanisms of hair cell renewal. Dev. Neurobiol. 67, 637–654.
Houweling, A.C., Dildrop, R., Peters, T., Mummenhoff, J., Moorman, A.F.M., Rüther, U., Christoffels, V.M., 2001. Gene and cluster-specific expression of the *Iroquois* family members during mouse development. Mech. Dev. 107, 169–174.
Hu, M., Easter, S.S., 1999. Retinal neurogenesis: the formation of the initial central patch of postmitotic cells. Dev. Biol. 207, 309–321.
Itoh, M., Kudoh, T., Dedekian, M., Kim, C.H., Chitnis, A.B., 2002. A role for *iro1* and *iro7* in the establishment of an anteroposterior compartment of the ectoderm adjacent to the midbrain–hindbrain boundary. Development 129, 2317–2327.
Jin, Z., Zhang, J., Klar, A., Chédotal, A., Rao, Y., Cepko, C.L., Bao, Z.Z., 2003. Irx4-mediated regulation of Slit1 expression contributes to the definition of early axonal paths inside the retina. Development 130, 1037–1048.
Jowett, T., Lettice, L., 1994. Whole-mount in situ hybridizations on zebrafish embryos using a mixture of digoxigenin- and fluorescein-labelled probes. Trends Genet. 10, 73–74.
Krauss, S., Concordet, J.P., Ingham, P.H., 1993. A functionally conserved homolog of the *Drosophila* segment polarity gene *hh* is expressed in tissues with polarizing activity in zebrafish embryos. Cell 75, 1431–1444.
Kiernan, A.E., Pelling, A.L., Leung, K.K., Tang, A.S., Bell, D.M., Tease, C., Lovell-Badge, R., Steel, K.P., Cheah, K.S., 2005. Sox2 is required for sensory organ development in the mammalian inner ear. Nature 434, 1031–1035.
Kim, C.H., Bae, Y.K., Yamanaka, Y., Yamashita, S., Shimizu, T., Fujii, R., Park, H.C., Yeo, S.Y., Huh, T.L., Hibi, M., Hirano, T., 1997. Overexpression of *neurogenin* induces ectopic expression of HuC in zebrafish. Neurosci. Lett. 239, 113–116.
Korzh, V., Sleptsova, I., Liao, J., He, J., Gong, Z., 1998. Expression of zebrafish bHLH genes ngn1 and nrd defines distinct stages of neural differentiation. Dev. Dyn. 213, 92–104.
Lecaudey, V., Anselme, I., Dildrop, R., Ruther, U., Schneider-Maunoury, S., 2005. Expression of the zebrafish *Iroquois* genes during early nervous system formation and patterning. J. Comp. Neurol. 492, 289–302.
Leyns, L., Gómez-Skarmeta, J.L., Dambly-Chaudière, C., 1996. iroquois: a prepattern gene that controls the formation of bristles on the thorax of *Drosophila*. Mech. Dev. 59, 63–72.
Lun, K., Brand, M., 1998. A series of no isthmus (noi) alleles of the zebrafish *pax2.1* gene reveals multiple signaling events in development of the midbrain–hindbrain boundary. Development 125, 3049–3062.
McNeill, H., Yang, C.H., Brodsky, M., Ungos, J., Simon, M.A., 1997. *mirror* encodes a novel PBX-class homeoprotein that functions in the definition of the dorso-ventral border of the *Drosophila* eye. Genes Dev. 11, 1073–1082.
Monsoro-Burq, A.H., Fletcher, R.B., Harland, R.M., 2003. Neural crest induction by paraxial mesoderm in *Xenopus* embryos requires FGF signals. Development 130, 3111–3124.
Morita, T., Nitta, H., Kiyama, Y., Mori, H., Mishina, M., 1995. Differential expression of two zebrafish *emx* homeoprotein mRNAs in the developing brain. Neurosci. Lett. 198, 131–134.
Okuda, Y., Yoda, H., Uchikawa, M., Furutani-Seiki, M., Takeda, H., Kondoh, H., Kamachi, Y., 2006. Comparative genomic and expression analysis of group B1 sox genes in zebrafish indicates their diversification during vertebrate evolution. Dev. Dyn. 235, 811–825.
Parinov, S., Kondrichin, I., Korzh, V., Emelyanov, A., 2004. Tol2 transposon-mediated enhancer trap to identify developmentally regulated zebrafish genes in vivo. Dev. Dyn. 231, 449–459.
Peters, T., Dildrop, R., Ausmeier, K., Ruther, U., 2000. Organization of the mouse *Iroquois* homeobox genes in two clusters suggest a conserved regulation and function in vertebrate development. Genome Res. 10, 1453–1462.
Pfeffer, P.L., Gerster, T., Lun, K., Brand, M., Busslinger, M., 1998. Characterization of three novel members of the zebrafish Pax2/5/8 family: dependency of Pax5 and Pax8 expression on the Pax2.1 (noi) function. Development 125, 3063–3074.
Riley, B.B., Phillips, B.T., 2003. Ringing in the new ear: resolution of cell interactions in otic development. Dev. Biol. 261, 289–312.
Sahly, I., Andermann, P., Petit, C., 1999. The zebrafish *eya1* gene and its expression pattern during embryogenesis. Dev. Genes Evol. 209, 399–410.
Sarrazin, A.F., Villablanca, E.J., Nunez, V.A., Sandoval, P.C., Ghysen, A., Allende, M.L., 2006. Proneural gene requirement for hair cell differentiation in the zebrafish lateral line. Dev. Biol. 295, 534–545.
Seo, H.C., Drivenes, O., Fjose, A., 1998. A zebrafish Six4 homologue with early expression in head mesoderm. Biochim. Biophys. Acta 1442, 427–431.
Schreiber-Agus, N., Horner, J., Torres, R., Chiu, F.C., De Pinho, R.A., 1993. Zebrafish *myc* family and *max* genes: differential expression and oncogenic activity throughout vertebrate evolution. Mol. Cell. Biol. 13, 2765–2775.
Schlosser, G., 2005. Evolutionary origins of vertebrate placodes: insights from developmental studies and from comparisons with other deuterostomes. J. Exp. Zoolog. B. Mol. Dev. Evol. 304, 347–399.
Schlosser, G., 2006. Induction and specification of cranial placodes. Dev. Biol. 294, 303–351.
Schlosser, G., Ahrens, K., 2004. Molecular anatomy of placode development in *Xenopus laevis*. Dev. Biol. 271, 439–466.
Trevarrow, B., Marks, D.L., Kimmel, C.B., 1990. Organization of hindbrain segments in the zebrafish embryo. Neuron 4, 669–679.
Williams, J.A., Barrios, A., Gatchalian, C., Rubin, L., Wilson, S.W., Holder, N., 2000. Programmed cell death in zebrafish rohon beard neurons is influenced by TrkC1/NT-3 signaling. Dev. Biol. 226, 220–230.
Wang, X., Emelyanov, A., Sleptsova-Friedrich, I., Korzh, V., Gong, Z., 2001. Expression of two novel zebrafish *iroquois* homologues (*ziro1 and ziro5*) during early development of axial structures and central nervous system. Mech. Dev. 105, 191–195.
Westerfield, M., 1994. The Zebrafish Book: guide for the laboratory use of the Zebrafish (Danio rerio). 2.1 Ed. University of Oregon Press, Eugene, OR.
Woo, K., Fraser, S.E., 1998. Specification of the hindbrain fate in the zebrafish. Dev. Biol. 197, 283–296.
Zou, D., Silvius, D., Fritzsch, B., Xu, P.X., 2004. Eya1 and Six1 are essential for early steps of sensory neurogenesis in mammalian cranial placodes. Development 131, 5561–5572.